Chapter 4

Strong Hydrogen Bonds - Hydrogen Dihalides

The results of the study on hydrogen dihalide anions of the type XHY^- (X, Y = halogen atoms) are presented in this chapter. These are the first gas phase infrared studies performed on these systems. The first section focuses on the infrared spectroscopy of the hydrogen homodihalide anions $Br(HBr)_n^-$ ($n = 1, 2, 3$) and $Br(DBr)_n^-$ ($n = 1, 2$).[73,74] The three atomic hydrogen homodihalides XHX^- ($X = Br$) are characterized by a symmetrically situated hydrogen atom between two halogen atoms. The spectra measured by infrared multiphoton photodissociation spectroscopy (IRMPD) are compared with the vibrational predissociation spectra (VPD) measured with the messenger atom technique and with theoretical predictions. Isotope effects will be presented in this chapter as well. Furthermore, the solvation effects on hydrogen bonding by addition of HBr units are discussed. The heterodihalides $BrHI^-$ and $BrDI^-$ will be presented in the second section of this chapter. These ions are characterized by an asymmetrically located hydrogen atom, closer to the iodide atom. The infrared spectra of these anions were measured with both methods mentioned previously, namely multiphoton photodissociation and the messenger atom technique and the results obtained with both methods will be discussed. The results obtained from the VPD spectra of $BrHBr^- \cdot Ar$, the IRMPD spectra of $Br(HBr)_n^-$ ($n = 1, 2, 3$) and from the IRMPD and VPD spectra of $BrHI^-$ and $BrDI^-$ were published previously.[73–75] Additional unpublished results on the IRMPD spectrum of $BrHBr^-$ and $Br(DBr)_n^-$ (n=1, 2) and the VPD spectra of $BrDBr^- \cdot Ar$ which offer supplementary informations and help the assignments are presented in this chapter.

4.1 Gas Phase Infrared Spectroscopy of Symmetric Hydrogen Dihalide Anions as a Function of Size: The Effect of Solvation on Hydrogen-Bonding in $Br(HBr)^-_{1,2,3}$ clusters.

$BrHBr^-$ and $BrDBr^-$ have been extensively studied in rare gas matrices.[76–79] The experiments revealed four bands which were attributed to the antisymmetric stretch ν_3, which involves the motion of the H-atom between the two bromide atoms, and to combination bands involving the antisymmetric stretch with the symmetric stretch $\nu_3 + n\nu_1$. The symmetric stretch ν_1 corresponds to the movement of the heavy halogen atoms. In these experiments, the frequency of the ν_3 stretch was located in the range from 646 to 741 cm^{-1} depending on the matrix environment. Experimental[76–79] and theoretical studies[80] suggested a linear geometry with the H atom placed symmetrically between the two bromide atoms ($D_{\infty h}$). The CCSD(T)/aug'-cc-pVTZ predicted $H - Br$ distance in $BrHBr^-$ of 1.703 Å was calculated by Del Bene and Jordan.[80] Significant negative anharmonicity in the ν_3 mode was experimentally observed in matrix experiments,[77–79] revealed by the large deuterium shift for the ν_3 mode ($\nu_{3_{BrHBr^-}}/\nu_{3_{BrDBr^-}} = 1.47$), which exceeded the harmonic value ($\approx \sqrt{2}$). This prediction is supported by theory.[80] In contrast, a positive anharmonicity is observed in the Ar-matrix experiments[77,78] for the ν_1 mode indicated by a smaller separation between the bands ($\nu_3 + 2\nu_1$) and ($\nu_3 + \nu_1$) than between ($\nu_3 + \nu_1$) and ν_3. Anharmonic CCSD(T)/aug'-cc-pVTZ calculations performed on $BrHBr^-$ and $BrDBr^-$[80] predict 731 cm^{-1} for the antisymmetric stretch frequency. The calculations considered the isolated systems. However, no gas phase infrared spectra were previously measured for these systems. The $BrHBr^-$ dissociation energy is 0.93 eV,[81] making $BrHBr^-$ and $BrDBr^-$ good model systems for the study of strong hydrogen bonds.

Although a large number of experimental studies were performed on $BrHBr^-$, no infrared spectra are available for the larger systems $Br(HBr)^-_n$ ($n = 2, 3$). Similar systems such as $F^-(HF)_{2,3}$ and $Cl^-(HCl)_{2,3}$ anions have been previously studied by *ab initio* calculations[82–85] and matrix spectroscopy.[86] These studies predicted C_{2v} and C_{3v} geometries for the complexes with $n = 2$ and $n = 3$, respectively, with the hydrogen atom asymmetrically placed between the heavy atoms, closer to the terminal atoms.

4.1.1 Experiment

In the experiments presented in this thesis, $Br(HBr)^-_{n=1,2,3}$ and $Br(DBr)^-_{1,2}$ were produced with the electron impact source (see also Section 2.1.3). The molecular beam is formed from a gas mixture of 4 % pure HBr or DBr gas in Ar which is expanded through a pulsed valve with a 78 μm diameter oriffice, running at 20 Hz. The backing pressure was between 2 and 5 bar. Negative ions are produced by dissociative electron attachment of HBr as described in Section 2.1.3. Br^- ions are cooled in the expansion and can cluster with other HBr or DBr molecules. The general measurement procedure was already described in Chapter 2. In the experiments presented here, the trap was filled with 30 μbar He at temperatures below 70 K. For the IRMPD experiments on the symmetric hydrogen dihalides, $ZnSe$ optics (three windows and a 600 mm focal length lens) were used. For the VPD spectra of $BrHBr^- \cdot Ar$ (and $BrDBr^- \cdot Ar$) one $ZnSe$ window and three KBr optics (two windows and one 480 mm focal length lens) were used. The transmision efficiency of both materials is shown in Appendix B. 80 mJ per FELIX macropulse, measured before the $ZnSe$ (KBr) optics, was the maximum pulse energy used in these experiments. The low transmission of the $ZnSe$ optics (<50%) below 6 μm and above 17 μm (see Appendix B) limited the scanning range.

4.1.2 $BrHBr^-$

Multiphoton Dissociation Spectrum

The first IR spectrum for the $BrHBr^-$ anion was measured at the FELIX facility in the region between 625 and 1700 cm^{-1} with the IRMPD technique. The range of the spectrum which showed infrared activity, between 1460 and 1700 cm^{-1} (6.85 to 5.88 μm), is presented in Figure 4.1. The spectrum reveals one weak band at 1558 cm^{-1}. No depletion of the parent ion is observed. This can be explained by the instability of the ion source which produces oscillations in the parent ion signal on the order of 10% (see scale on the right side of the Figure 4.1) and hides the depletion. The low transmission efficiency of the $ZnSe$ optics (see Appendix B) reduces the intensity of the laser in this frequency region. Based on previous infrared experiments in matrices[76,77,79] which assigned the fundamental stretch of the H-atom around 730 cm^{-1}, the absorption band at 1558 cm^{-1} was attributed to the overtone of the antisymmetric stretch ν_3 (see also Reference[73]). The high frequency value of the assigned overtone was explained by the negative anharmonicity of the ν_3 mode,[73,80] which causes the overtone to appear at a frequency larger than twice the fundamental

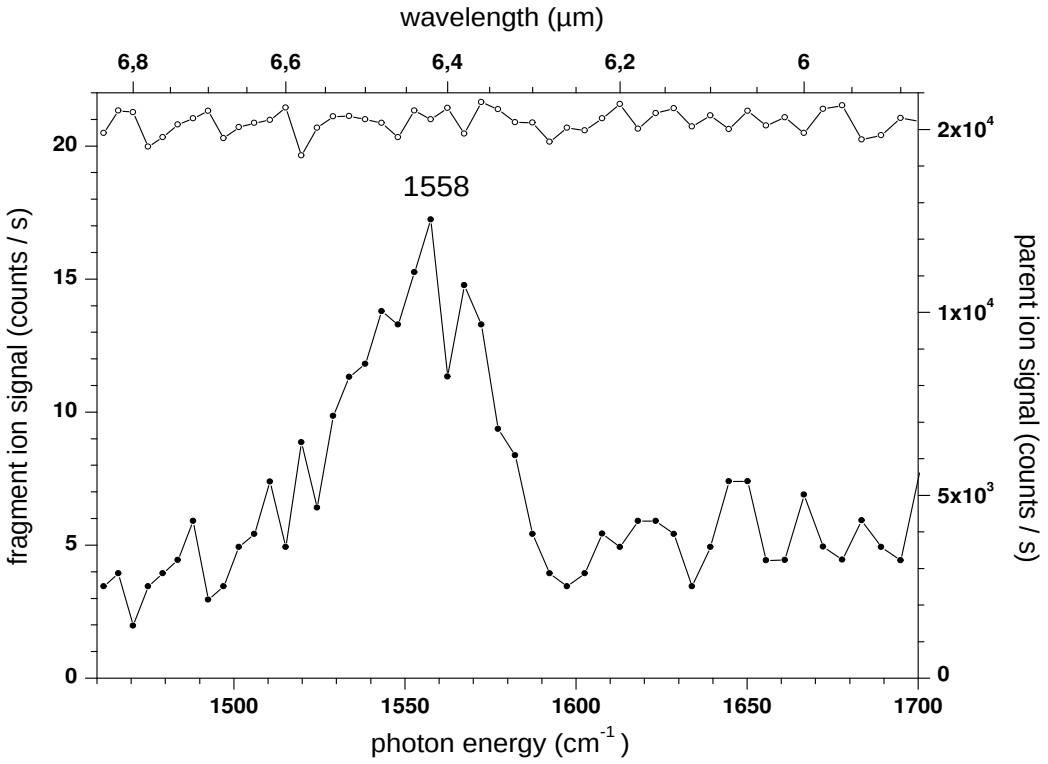

Figure 4.1: The first multiphoton infrared spectrum of $BrHBr^-$ anion (solid dots). The peak was assigned to the first overtone of the antisymmetric stretch ν_3. The parent ion signal is also presented (open dots). The scale for the fragment ion signal is shown on the left side, whereas for the parent ion signal is on the right side of the graph.[73]

frequency. No absorption bands were observed in the region around 800 cm^{-1}, where the fundamental of the ν_3 stretch is expected.

Predissociation Spectra

The dissociation energy of the $BrHBr^-$ anion is 0.93 eV and thus, 5 to 12 photons are necessary in order to fragment this ion. To circumvent problems related to multiphoton transitions, an Ar atom was attached to the ion and the infrared spectrum of the $BrHBr^- \cdot Ar$ complex was measured by using the messenger atom technique. The spectrum is shown in Figure 4.2 in the region from 610 to 1710 cm^{-1} (5.85 to 16.39 μm). The positions of the bands and their widths are listed in Table 4.1. The spectrum is scaled to the field-free background and plotted on logarithmic scale. The depletion intensities are given by $-ln(c/c_0)$, where c/c_0 is the depletion signal read from the spectrum. Here, it is considered that all the complexes vibrationally excited by each micropulse dissociate before the next micropulse 1 ns later, so that there is a steadily decreasing number of ions interacting with successive micropulses.[75] Under

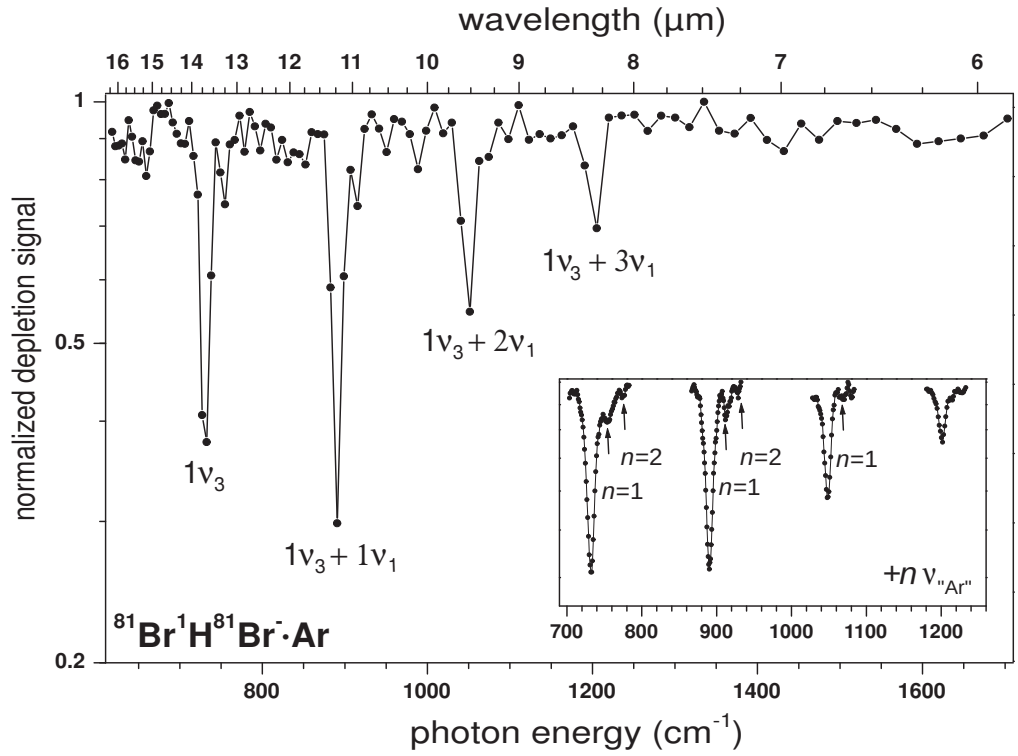

Figure 4.2: The vibrational predissociation spectrum of $BrHBr^- \cdot Ar$. The depletion ion signal intensity is shown on a logarithmic scale. Higher resolution spectra were recorded at each position of the peaks and are shown in the inset.[74]

these circumstances, $-ln(c/c_0)$ is proportional to the transition strength. The spectrum was measured with a step size of 0.1 μm. Higher resolution spectra, i.e., smaller step sizes of 0.01 and 0.02 μm and with increased number of shots per data point, were measured in the regions with infrared activity. These high resolution depletion spectra are presented in the inset of Figure 4.2.

The VPD spectrum of $BrHBr^- \cdot Ar$ (Figure 4.2) reveals four strong peaks at 733, 890, 1048 and 1202 cm^{-1}. The peak widths are between 10 and 15 cm^{-1} and are on the order of the FELIX bandwidth. The separation between the peaks remains approximately constant with values between 158 and 154 cm^{-1}, decreasing slightly at higher frequencies. Lower intensity bands are observed at 754, 775, 911, 929 and 1070 cm^{-1} which are best seen in the high resolution spectrum (see the inset of Figure 4.2).

Comparison of the gas phase infrared spectrum with the matrix spectra[76,77,79] helps the assignment of the peaks (see Table 4.2). Thus, the first peak at 733 cm^{-1} is attributed to the antisymmetric stretch. The following bands are assigned to combinations of the symmetric stretch ν_1 with the ν_3 antisymmetric stretch ($\nu_3 + n\nu_1$). The

Table 4.1: Peak assignment and experimental frequencies obtained from the predissociation spectra of $BrHBr^- \cdot Ar$ and $BrDBr^- \cdot Ar$. The peak widths and the calculated frequencies[80] are listed as well.

	$BrHBr^- \cdot Ar$			$BrDBr^- \cdot Ar$		
	Experiment		Theory	Experiment		Theory
Assignment	Frequency cm^{-1}	Width cm^{-1}	Frequency cm^{-1}	Frequency cm^{-1}	Width cm^{-1}	Frequency cm^{-1}
$1\nu_3$	733	15	731			479
$1\nu_3 + 1\nu_{"Ar"}$	754					
$1\nu_3 + 2\nu_{"Ar"}$	775					
$1\nu_3 + 1\nu_1$	890	13	893	668	16	647
$1\nu_3 + 1\nu_1 + 1\nu_{"Ar"}$	911			694		
$1\nu_3 + 1\nu_1 + 2\nu_{"Ar"}$	929					
$1\nu_3 + 2\nu_1$	1048	11	1054	830	11	812
$1\nu_3 + 2\nu_1 + 1\nu_{"Ar"}$	1070			850		
$1\nu_3 + 3\nu_1$	1202	10	1212	989	8	972

decrease of the spacing between the combination bands (158 to 154 cm^{-1}) supports the previous prediction of a positive anharmonicity of the ν_1 mode. The fundamental ν_1 frequency can be estimated from the spacing of the combination bands, $\nu_3 + n\nu_1 - \nu_3$, yielding 158 cm^{-1}. The CCSD(T)/aug'-cc-pVTZ theoretical treatment of the $XH(D)X^-$ systems with $X = F, Cl, Br$ performed by Del Bene and Jordan[80] on a two dimensional (2D) potential energy surface (PES) are in very good agreement with the experimental matrix and gas phase results (see Tables 4.1 and 4.2). These calculations predict 165 cm^{-1} for $(\nu_1 + \nu_3) - \nu_3$, 24 cm^{-1} smaller than the ν_1 fundamental (189 cm^{-1}). This difference indicates that excitation of the antisymmetric stretch reduces the symmetric stretch frequency (see Table 4.2). The appearance of the intense combination bands in the IR spectrum of $BrHBr^- \cdot Ar$ indicates that the standard one dimensional (1D) treatment using the harmonic approximation is inadequate for these systems regardless of the level of the theory and a 2D treatment is necessary as predicted by theory.[80]

The depletion peak intensities in the gas phase infrared spectrum are different than observed in the matrix spectra,[76–79] where the fundamental of the antisymmetric stretch is by a factor of two more intense than the first combination band $1\nu_3+1\nu_1$. In the gas phase IR spectrum, the combination band $\nu_3+\nu_1$ has a slightly higher intensity than the fundamental of the antisymmetric stretch ν_3. Factors that can influence the intensity of the bands in the IR spectrum are the FELIX power and bandwidth and the

Table 4.2: Comparison of the experimental gas phase, matrix and calculated vibrational frequencies for $BrHBr^-$ and $BrDBr^-$. The frequencies of the combination bands are presented as $\nu_3 + n\nu_1 - \nu_3$ values. For $BrDBr^-$, the frequency difference to the previous values of ν_3 or $\nu_3 + \nu_1$ is presented in square brackets in order to make the comparison with the gas phase values easier, where the ν_3 stretch could not be observed because it was red-shifted below the detection region.

Assignment	Gas phase	Matrix			Theory[d]
		Ne[a]	Ar[b]	Kr[c]	
	cm^{-1}	cm^{-1}	cm^{-1}	cm^{-1}	cm^{-1}
$BrHBr^- \cdot Ar$					
$1\nu_3$	733	741	728	687	731
$1\nu_3 + 1\nu_1$	+157	+163	+164	+158	+162
$1\nu_3 + 2\nu_1$	+315		+325	+313	
$1\nu_3 + 3\nu_1$	+469			+466	
$BrDBr^- \cdot Ar$					
$1\nu_3$		507	498	466	479
$1\nu_3 + 1\nu_1$	668	667 [+160]	668 [+170]	629 [+163]	647 [+168]
$1\nu_3 + 2\nu_1$	+160		+335 [+165]	+323 [+160]	+333 [+165]
$1\nu_3 + 3\nu_1$	+316				+493 [+325]

[a]Ref.[76], [b]Ref.[77], [c]Ref.[79], [d]Ref.[80]

ion predissociation rate. FELIX was optimized such that the power and bandwidth change as little as possible over the frequency scanning range. For the dissociation rate to affect the peak intensities, the dissociation lifetime must be on the order of few μs, since this is the time scale for the collisions between the trapped ions and the He buffer gas atoms in the trap. The ions are extracted 1 ms after the irradiation pulse, so it can be assumed that the photoexcited ions have either dissociated or were collisionally quenched before extraction. For the relative peak intensities, it seems that the dissociation rate increases with the excitation of the symmetric stretch. This can be due to the excess energy above the dissociation threshold which determines the dissociation rate. Another possibility is the mode-specific predissociation rate, where ν_1 excitation promotes the dissociation more efficiently than ν_3 excitation.[74]

Beside the high intensity peaks, in the high resolution spectra shown in the inset of Figure 4.2 additional bands are observed at a separation of approximately 20 cm^{-1} from the main peaks. These low frequency bands are attributed to modes involving the Ar atom motion $+n\ \nu_{Ar}$, i.e., to combination modes of the IR active mode with the low frequency intermolecular $BrHBr^- \cdot Ar$ modes. Side bands where observed

only in the high energy region of the peaks confirming that the complex ions are originally in their vibrational ground state. These types of van der Waals modes were observed also in IR spectra of systems such as $benzene - Ar, Ne$.[87]

The assignment presented above is supported by the IR spectrum of the deuterium substituted complex. The infrared spectrum of the $BrDBr^- \cdot Ar$ anion in the range from 600 to 1400 cm^{-1} is shown in Figure 4.3. Spectra with smaller step sizes are shown in the inset of the figure. Three bands are observed at 668, 830 and 989 cm^{-1}. The peak widths vary from 8 to 16 cm^{-1} similar to the bandwidth of the laser. The assignment of the bands of the $BrDBr^- \cdot Ar$ anion spectrum is performed in a similar way to the spectrum of the $BrHBr^- \cdot Ar$ complex, based on matrix spectra,[76,77,79] calculated 2D anharmonic frequencies[80] and on the expected isotope shifts due to deuterium substitution. The three peaks are assigned to combination bands of the antisymmetric stretch and the symmetric stretch $\nu_3 + n\nu_1$ (n=1-3) (Table 4.1). The fundamental frequency of the antisymmetric stretch ν_3 is calculated at 479 cm^{-1}, but it could not be observed in the experimental spectrum because it lies outside of the observation window. The separation between $1\nu_3 + 2\nu_1$ and $1\nu_3 + 1\nu_1$ (160 cm^{-1}) is

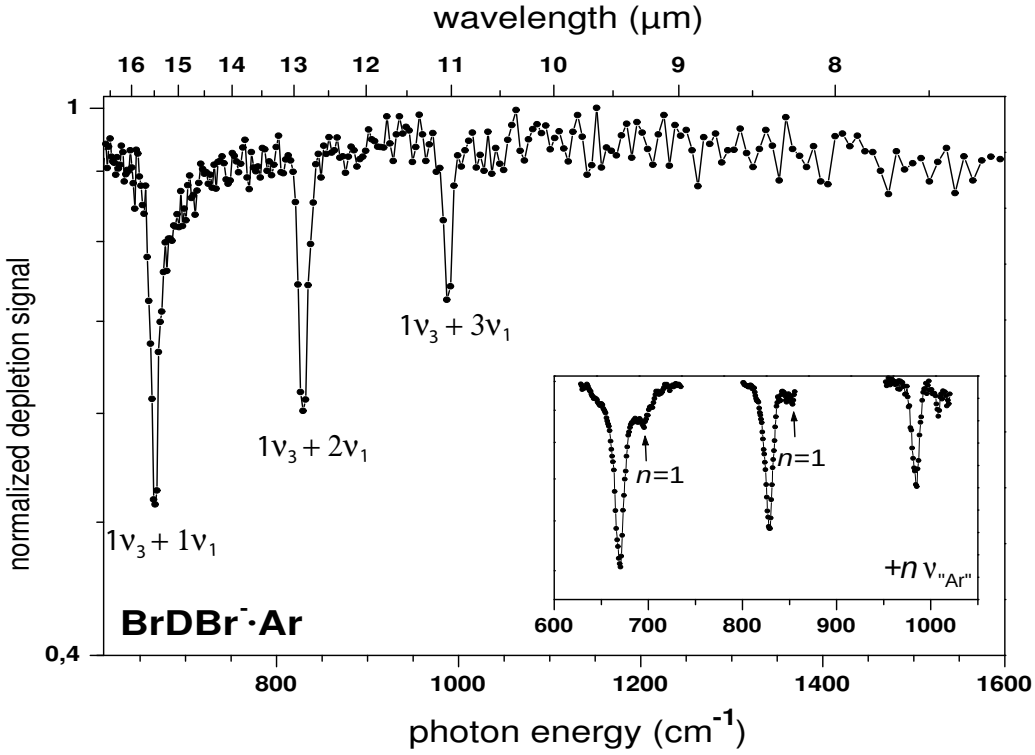

Figure 4.3: The VPD spectrum of $BrDBr^- \cdot Ar$. The ion depletion signal intensity is shown on a logarithmic scale. Higher resolution spectra were measured at each position of the peaks and are shown in the inset.

larger than between the bands $1\nu_3 + 3\nu_1$ and $1\nu_3 + 2\nu_1$ (156 cm^{-1}) which supports the assignment of positive anharmonicity (lowering of the distance between vibrational levels with increasing energy) in the ν_1 mode as observed in matrix experiments[76–79] (see Table 4.2) and in $BrHBr^- \cdot Ar$. The symmetric stretch does not involve the motion of the hydrogen atom and therefore, no frequency shift upon deuteration is expected. The calculated value for the fundamental of the symmetric stretch for $BrDBr^-$ is 189 cm^{-1} very close to the ν_1 value of $BrHBr^-$ of 188 cm^{-1}. The experimental isotopic shift is in the range from 1.33 to 1.22, decreasing with increasing energy. The same trend is supported by the CCSD(T)/aug'-cc-pVTZ calculations.[80] As in the case of the $BrHBr^- \cdot Ar$ complex, vibrations involving the Ar atom are observed (see inset of the Figure 4.3) at 694 and 849 cm^{-1}, $\approx$ 20 cm^{-1} higher in frequency than the main peaks.

Multiphoton Dissociation Spectra

After the VPD experiments, the IRMPD spectrum of $BrHBr^-$ anion was measured again with higher laser intensity ($\approx$ 80 mJ energy per macropulse) in order to overcome the high dissociation energy of 0.93 eV[81] of the molecule. The spectrum is shown in Figure 4.4 (lower trace). For comparison, the VPD spectrum of the $BrHBr^- \cdot Ar$ is shown as well (upper trace). Some similarities are observed between the VPD and the IRMPD spectra as shown by the pairs of peaks with the same labels. However, the multiphoton spectrum presents additional absorption bands. Many of the peaks in the IRMPD spectrum appear as group of bands. The positions of all observed bands are listed in Table 4.3. Peaks F', G' and H' have no corresponding bands in the VPD spectrum and show here a high intensity. The separations between the peaks maxima of E', G' and H' and between the peaks maxima of F' located at 1274 cm^{-1} and the second band in G' positioned at 1424 cm^{-1} are in the range from 149 to 152 cm^{-1} and suggest combinations with the low frequency ν_1 mode. No peak at 1558 cm^{-1}, as observed in the first IRMPD spectrum, appears in this spectrum.

An assignment of the multiphoton spectrum is less straightforward compared to the assignment of the VPD spectrum of $BrHBr^- \cdot Ar$, in particular in the absence of calculations which consider the multiphotonic nature of the excitation process. Only a qualitative interpretation of the experimental data is presented here and tentative assignments of the bands are listed in Table 4.3. The bands in the IRMPD spectrum which appear at similar frequencies as the ones in the VPD spectrum can be assigned accordingly. As a consequence, the bands at 753, 880, 1038 and 1206 cm^{-1} are attributed to the fundamental of the antisymmetric stretch and to combinations of

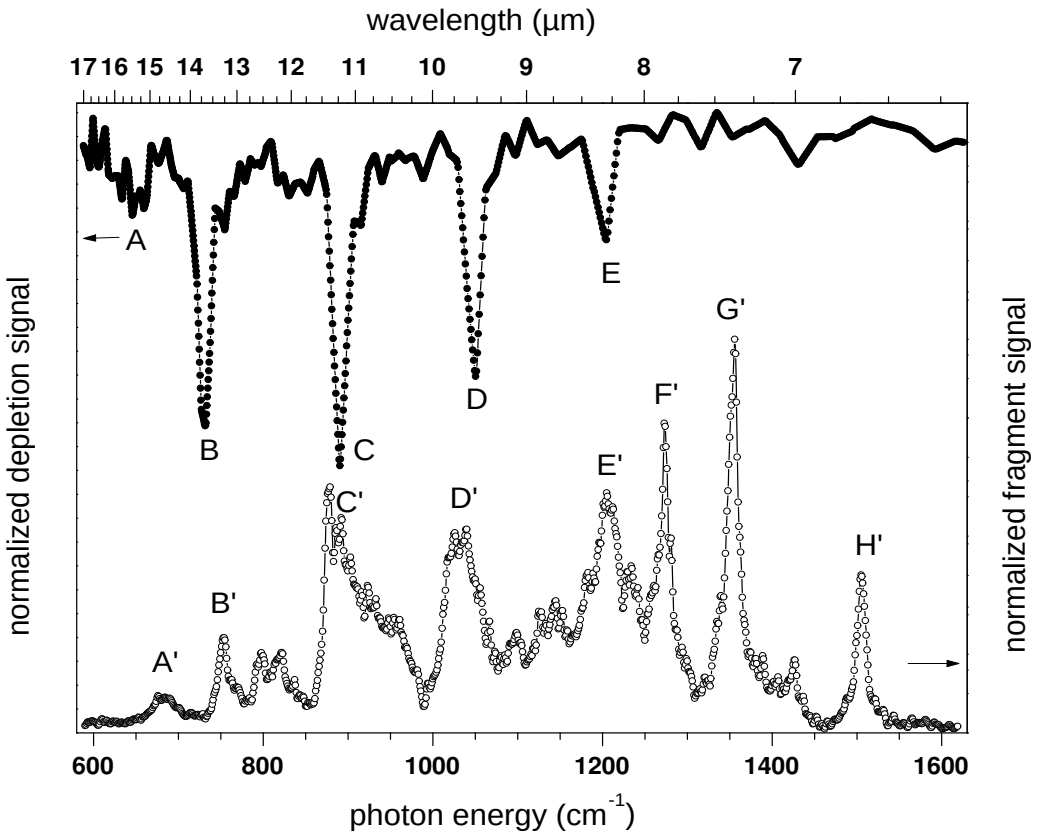

Figure 4.4: The infrared multiphoton photodissociation spectrum of $BrHBr^-$ (open circles). For comparison, the vibrational predissociation spectrum of the $BrHBr^- \cdot Ar$ complex is shown in the upper trace (closed circles). The peak positions are listed in Table 4.3.

the antisymmetric stretch with the symmetric stretch $\nu_3 + n\nu_1$, with $n = 1 - 3$. The separation between the bands E', G' and H' of $\approx 150\ cm^{-1}$ is similar to the separation between the peaks in the VPD spectrum. Thus, peaks G' and H' are assigned to combinations bands of peak E' with the symmetric stretch, namely to $\nu_3 + 4\nu_1$ and $\nu_3 + 5\nu_1$, respectively. Alternatively, peak H' can be tentatively assigned to the first overtone of the antisymmetric stretch. Based on the spacing between peaks F' and G' at 1424 cm^{-1}, the later can be assigned to a combination of peak F' with the symmetric stretch.

The relative peak intensities in the IRMPD spectrum are difficult to interpret. The last peaks F', G', H' present higher intensities than the rest of the bands even though they are tentatively assigned to combinations with high order overtones of the symmetric stretch. This could be explained by a lower number of photons that need to be absorbed in this high energy region of the spectrum in order to reach

Table 4.3: Tentative peak assignment for the infrared multiphoton dissociation (IRMPD) spectrum of $BrHBr^-$. The normalized intensities of the IRMPD spectrum are listed as well. For comparison also the positions of the absorption bands in the VPD spectrum of the $BrHBr^- \cdot Ar$ together with their assignments are presented. Possible two photon transitions are indicated in brackets as 2ph. together with the label of the one photon band from which these might result.

	$BrHBr^-$		$BrHBr^- \cdot Ar$	
Peak	Frequency cm^{-1}	Relative Intensity	Frequency cm^{-1}	Assignment
A'	682	0.09	653	$1\nu_2$ (2ph. H')
B'	753	0.24	733	$1\nu_3$ (2ph. G')
	797	0.20		
	820	0.20		
C'	880	0.62	890	$1\nu_3 + 1\nu_1$
	891	0.54		
	929	0.37		
	957	0.29		
D'	1025	0.51		
	1038	0.51	1048	$1\nu_3 + 2\nu_1$
	1100	0.26		
	1128	0.31		
	1145	0.34		
E'	1206	0.61	1202	$1\nu_3 + 3\nu_1$
	1234	0.42		
F'	1274	0.79		
G'	1358	1.00		$1\nu_3 + 4\nu_1$
	1424	0.18		
H'	1507	0.4		$1\nu_3 + 5\nu_1$ ($2\nu_3$)

the dissociation limit. It is also interesting to observe that the intensity of the peak labeled as B', tentatively assigned here to the fundamental of the ν_3 stretch is low compared to peak B from the VPD spectrum. The low intensity of this band could also be explained by the same reason as above, i.e., a higher numbers of photons is necessary to be absorbed at these energies (753 cm^{-1}) in order to dissociate the ion. Finally, an absorption band A' at 682 cm^{-1} is observed in the IRMPD spectrum of the $BrHBr^-$ anion, its pair in the VPD spectrum possibly being the band A at 653 cm^{-1}. The intensity of peak A in the VPD spectrum is very low and no band was theoretically predicted at this frequency. One could assign this band to the fundamental of the bending mode, however, the bending mode was not observed in

the matrix spectra. The predicted harmonic value of the bending mode is 767 cm^{-1}, being by more than 100 cm^{-1} higher in frequency than the experimentally observed band A.

At the high laser intensities generated by FELIX, also multiple photon transitions in which two photons are resonant with a vibrational transition are possible. Considering this possibility, an alternative assignment for some of the bands is proposed. The first peak in the band B' located at 753 cm^{-1} can be attributed to a two photon transition of the band H' located at 1507 cm^{-1}. Additionally, the weak transition at 682 cm^{-1} can be attributed to a two photon transition of the band G' located at 1358 cm^{-1}.

For an assignment of the band F' as well as of other bands in the IRMPD spectrum and the understanding of the peak intensities, high level calculations which address the experiment directly are needed.

A similar relationship between the VPD and the IRMPD spectra was observed also for $BrHI^-$ and $BrDI^-$[75] (see Section 4.2). In the spectra of these systems some transitions in the VPD spectrum appear as groups of peaks in the IRMPD spectra. The additional bands in these groups of peaks were assigned to two photon transitions. The calculations preformed in the group of J. M. Bowman[75] for $BrHI^-$ and $BrDI^-$ predict high overtone excitations of all three modes (symmetric, antisymmetric and bending modes) up to $n = 5$. In these systems the highest intensity bands in the groups of peaks of the IRMPD spectrum were assigned in some cases to two photon transitions (rather than one photon).[75] The same multiple photon absorptions which are resonant with one vibrational transitions can be expected also in $BrHBr^-$. The calculations on $BrHI^-$ and $BrDI^-$ showed that Fermi resonances play an important role in the intensity of the peaks. A relative shift between pairs of peaks of the VPD and IRMPD spectra of up to 30 cm^{-1} is observed in $BrHI^-$ similar to the predicted shifts in $BrHBr^-$ based on the assignments presented here.

The IRMPD spectrum of the $BrDBr^-$ anion was measured as well. An even more complicated intensity pattern than in the case of the IRMPD spectrum of the $BrHBr^-$ anion is observed. Additional studies are necessary in order to understand the IRMPD spectrum of $BrDBr^-$.

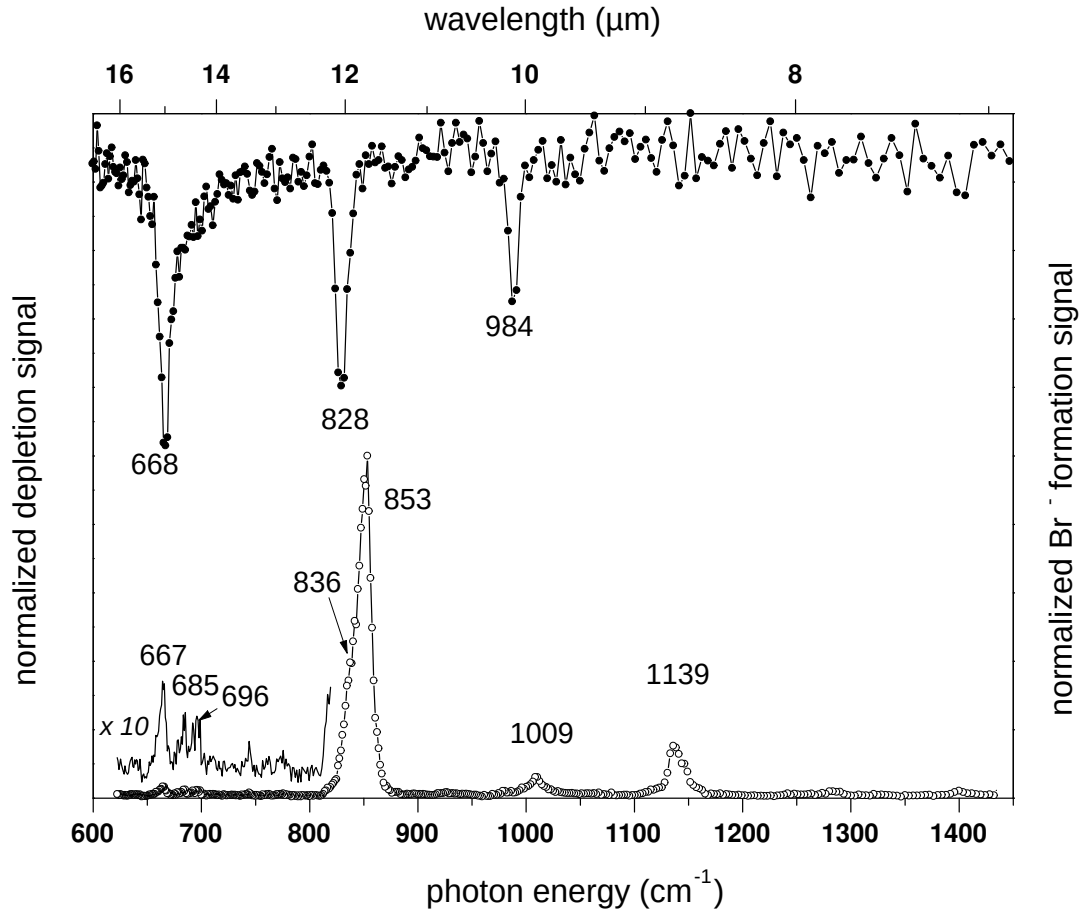

Figure 4.5: The IRMPD spectrum of the $BrDBr^-$ anion (open circles). For comparison, the vibrational predissociation spectrum of the $BrDBr^- \cdot Ar$ complex is shown in the upper trace (closed circles).

4.1.3 $Br(HBr)_{2,3}^-$ / $Br(DBr)_2^-$

Results

In order to understand the effect of solvation at addition of HBr units to the $BrHBr^-$ chromophore, the IRMPD spectrum of the $Br(HBr)_2^-$ and of the deuterated $Br(DBr)_2^-$ anions was measured between 600 and 1700 cm^{-1} (6 and 17 μm). The two spectra in the range from 825 to 1525 cm^{-1} for $Br(HBr)_2^-$ and from 600 to 1600 cm^{-1} for $Br(DBr)_2^-$ are shown in Figures 4.6 and 4.7, respectively. The spectra reveal a series of absorption bands. Their central frequencies are listed in Table 4.4.

The main dissociation channel is the loss of one HBr unit for $Br(HBr)_2^-$ and one DBr unit for $Br(DBr)_2^-$. A background signal of $BrHBr^-$ and $BrDBr^-$, respectively is produced through collision induced dissociation in the trap. The IR spectrum of $Br(HBr)_2^-$ shows six distinct peaks at 992, 1048, 1104, 1147, 1359 and

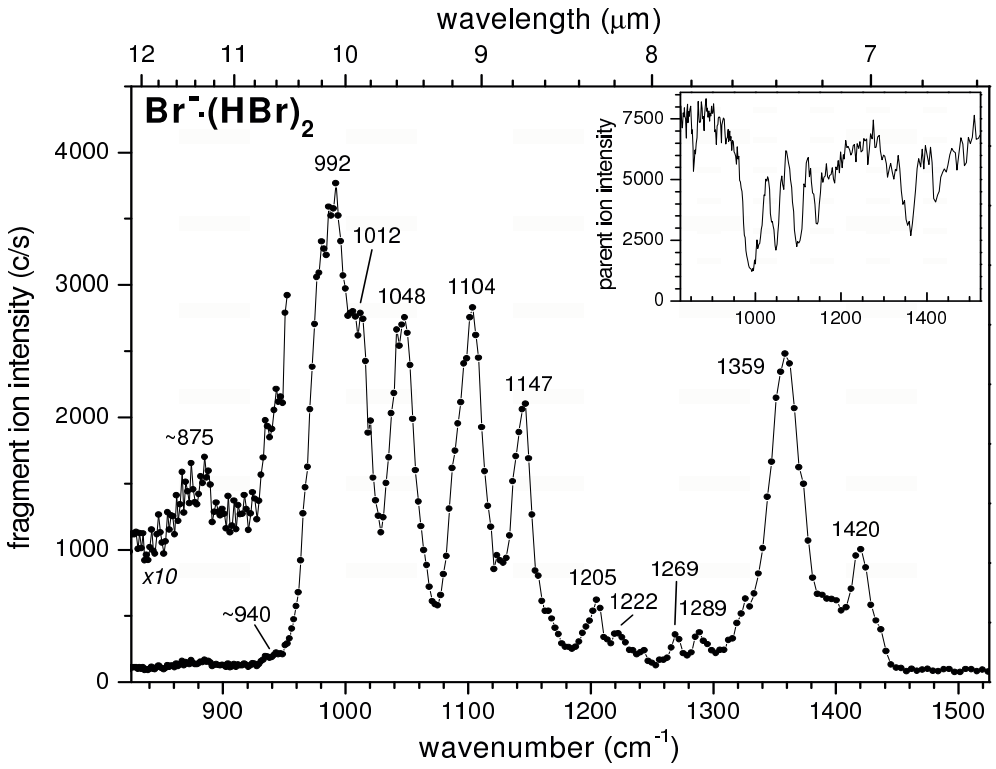

Figure 4.6: The infrared photodissociation spectrum of $Br(HBr)_2^-$. The position of the peaks in shown in the figure. The inset depicts the parent ion depletion signal as a function of the laser frequency.[73]

1420 cm^{-1}. The band at 992 cm^{-1} has a shoulder at 1012 cm^{-1} indicating an additional peak. Smaller peaks at 875, 1205, 1222, 1269 and 1289 cm^{-1} are also observed in the $BrHBr^-$ fragment ion spectrum. For $Br(HBr)_2^-$, the parent ion depletion spectrum is shown in the inset of Figure 4.6. A strong correlation between the parent and the fragment ion spectra is observed. At 992 cm^{-1}, the most intense peak in the $Br(HBr)_2^-$ spectrum, the parent ions are depleted by 85%, indicating that the depletion occurs not only in the focus of the laser beam but extends over the complete irradiated region of the trap. All absorption bands for $Br(HBr)_2^-$ and $Br(DBr)_2^-$ have peak widths larger than the bandwidth of the laser which in these experiments was 8-11 cm^{-1}. For $Br(HBr)_2^-$, the formation of Br^- (2 HBr loss) was also observed. However the ion intensity was less than 0.2% of the total photoproduct and no distinct features were observed in the spectrum.

The infrared spectrum of $Br(DBr)_2^-$ was measured by monitoring the fragment ion $BrDBr^-$ intensity at different laser attenuations as a function of FELIX frequency. Figure 4.7 shows the infrared spectra measured at -3 dB (red line, stars), -5 dB (blue line, dots) and -8 dB (black line, triangles). The most intense bands are found at 950,

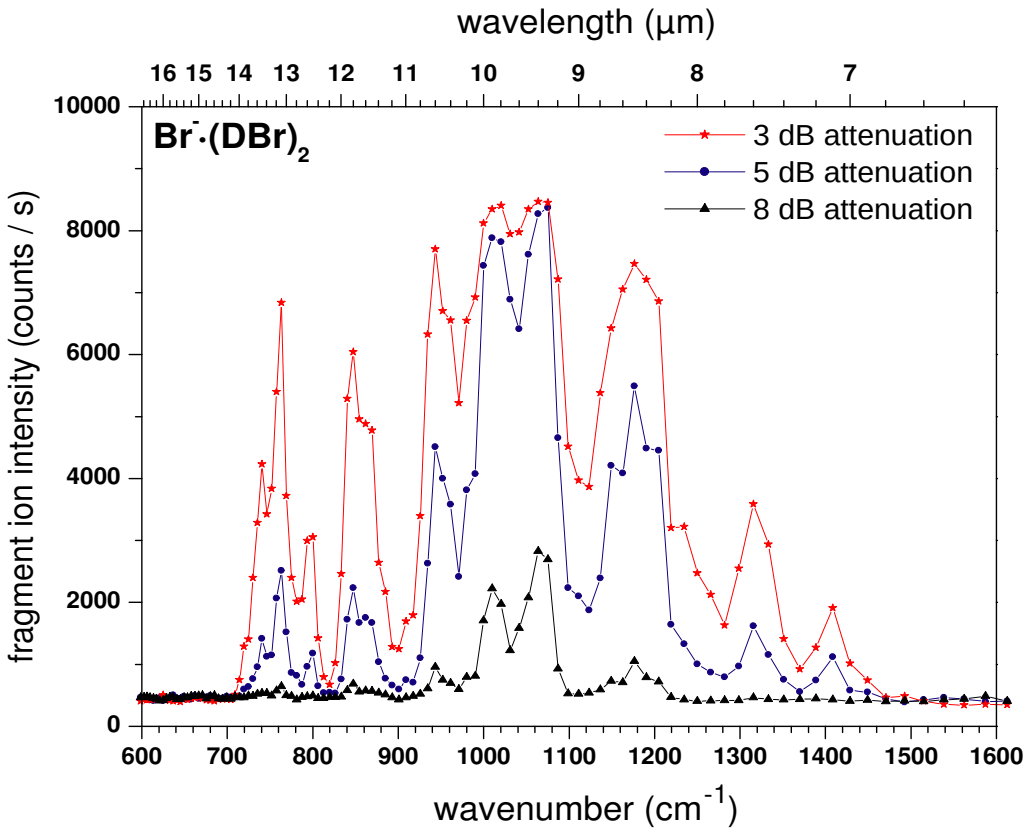

Figure 4.7: The infrared photodissociation spectrum of the $Br(DBr)_2^-$ anion recorded at different laser powers: -3 dB (red line, stars), -5 dB (blue line, dots) and -8 dB (black line, triangles). The positions of the peaks are listed in Table 4.4.

1014, 1067 and 1178 cm^{-1} with two shoulders at 1152 and 1201 cm^{-1} which indicate the presence of two additional bands. The two peaks at 1014 and 1067 cm^{-1} present the highest intensity in the spectrum, showing a large broadening at -3 and -5 dB due to saturation effects. The intensity of all other observed vibrational bands decreases strongly by laser attenuation. At -8 dB only six distinct features at 761, 848, 950, 1014, 1067 and 1178 cm^{-1} are observed.

Figure 4.8 shows the IR spectra of $Br(DBr)_2^-$ and $Br(HBr)_2^-$, where in the latter the peak positions were divided by 1.4 based on the harmonic isotope shift in order to see the corresponding peaks between the two spectra. The agreement between the two spectra based on the harmonic shift is not satisfactory. The corresponding peak intensities in $Br(DBr)_2^-$ and $Br(HBr)_2^-$ are very different as well. However, it needs to be considered that the radiation intensity is higher around 1000 cm^{-1} than at 700 cm^{-1}. Therefore, the peaks in $Br(DBr)_2^-$ around 700 cm^{-1} are less intense than the corresponding peaks in $Br(HBr)_2^-$ which are higher in energy. Also the transmitted

Table 4.4: Peak positions and normalized intensities for the IRMPD spectrum of $Br(HBr)_2^-$ and $Br(DBr)_2^-$.

$Br(HBr)_2^-$		$Br(DBr)_2^-$	
Peak position (cm^{-1})	Intensity	Peak position (cm^{-1})	Intensity
875	0.05	741	0.17
940	0.06	761	0.30
992	1.00	798	0.14
1012	0.74	848	0.27
1048	0.73	865	0.21
1104	0.75	950	0.54
1147	0.56	1014	0.94
1205	0.16	1067	1.00
1222	0.1	1152	0.50
1269	0.1	1178	0.66
1289	0.1	1201	0.53
1359	0.66	1318	0.19
1420	0.27	1408	0.13

radiation by the $ZnSe$ optics used for the $Br(HBr)_2^-$ measurements is low in the region below 700 cm^{-1} and above 1250 cm^{-1} which might lead to the fact that the peaks at $\approx$ 1400 cm^{-1} appear with a lower intensity. A better overlapped between the two spectra is observed when an isotope shift of $\approx$ 1.3, such as for systems with positive anharmonicity, is considered. If the reasonable isotope shifts of 1.3 to 1.34 are considered, the peaks at 992, 1012, 1048, 1104, 1147, 1359 and 1420 cm^{-1} in the $Br(HBr)_2^-$ anion IR spectrum would correspond to peaks 741, 761, 798, 865, 1067, 1014 cm^{-1} in $Br(DBr)_2^-$. The intensities of corresponding peaks in the two spectra are still far from similar.

Furthermore, the infrared spectrum of $Br(HBr)_3^-$ was measured between 6 and 16 μm (625 to 1666 cm^{-1}). The positions of the absorption bands are shown in Figures 4.9 and 4.10 and are listed in Table 4.5, together with normalized intensities. Two dissociation channels are observed, namely, the loss of one and two HBr units. Figure 4.9 depicts the $Br(HBr)_2^-$ fragment ion as a function of laser frequency. The macropulse energy was 25 mJ. Two absorption bands are observed at 888 and 979 cm^{-1}. At 888 cm^{-1} more than 80% of the parent ion is depleted as shown in the inset of the Figure 4.9. The width of this band is >30 cm^{-1} and is significantly larger than the laser bandwidth of 8-11 cm^{-1}. The broadening can be due to saturation effects. A constant background of fragment ion formed in the trap due to collision induced

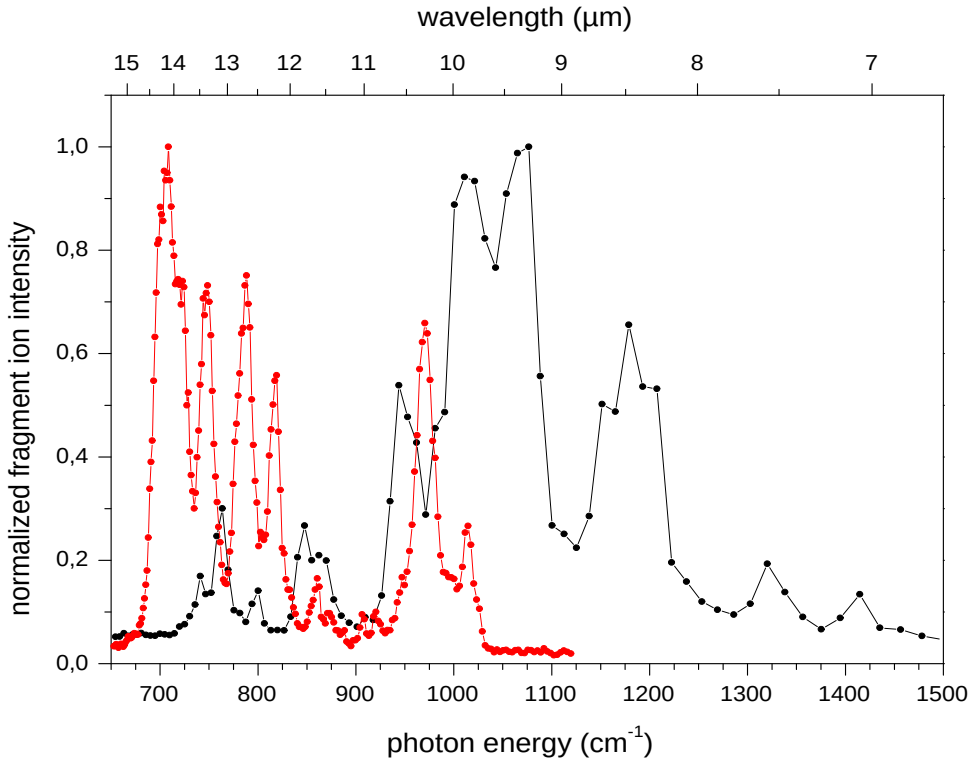

Figure 4.8: The infrared photodissociation spectrum of $Br(DBr)_2^-$ (black line) and $Br(HBr)_2^-$ (red line). The IR spectrum of $Br(HBr)_2^-$ was divided by 1.4, the harmonic isotope shift.

dissociation with the He atoms is observed. At the maximum of the band centered at 888 cm^{-1}, this background amounts to less than 10 % of the fragment ion signal. Loss of two HBr units is also observed at this energy (25 mJ /macropulse), but with a very low efficiency (less than 1% at 888 cm^{-1}).

At higher laser energies, 50 $mJ/macropulse$, the infrared spectrum is considerably different (shown in Figure 4.10). The parent ion depletion spectrum reveals a second band at 979 cm^{-1}. At 884 cm^{-1} 100 % of the parent ion is depleted. The IR spectrum which reveals the loss of one HBr unit (not shown) looks similar to the one recorded at lower laser power. A strong broadening of the band is observed which is attributed to saturation effects. The intensities of the absorption bands formed by the dissociation of two HBr units is increased at high laser energies. In contrast to the low laser energy spectrum a strong absorption band at 984 cm^{-1} is observed. This band nearly coincides with the 992 cm^{-1} infrared band in the $Br(HBr)_2^-$ spectrum and is therefore attributed to a sequential process which leads to the formation of $BrHBr^-$,

$$Br(HBr)_3^- \overset{nh\nu}{\rightarrow} Br(HBr)_2^- + HBr \overset{n'h\nu}{\rightarrow} BrHBr^- + HBr \qquad (4.1)$$

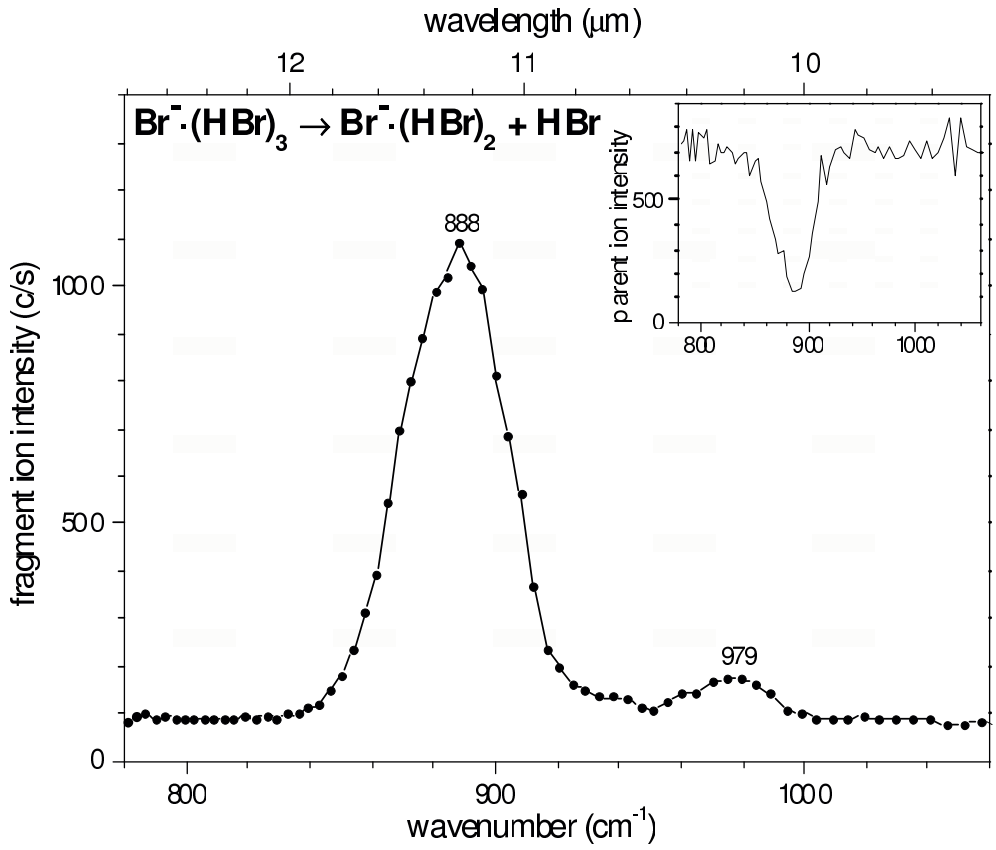

Figure 4.9: The infrared photodissociation spectrum of the $Br(HBr)_3^-$ anion. The $Br(HBr)_2^-$ fragment ions intensity was monitored as a function of the photon energy. The spectrum was recorded at a laser power of 25 mJ /macropulse. The inset presents the parent ion depletion spectra.[73]

when the laser frequency is resonant with a transition in both $Br(HBr)_3^-$ and $Br(HBr)_2^-$ anions. The small peaks in the region between 1000 and 1500 cm^{-1} appear at the same positions as in the IR spectrum of $Br(HBr)_2^-$. Therefore, these bands are attributed to photodissociation of the cluster with $n = 2$ formed in the ion trap through collision induced dissociation. The intensity of these peaks is consistent with the magnitude of the fragment ions observed in the trap without FELIX excitation, which are formed through collisions with the He atoms.

Discussions

A B3LYP/aug-cc-pVTZ theoretical treatment of $Br(HBr)_{2,3}^-$ was performed by N. Pivonka.[73] Geometry optimization as well as vibrational frequencies were calculated. The structures for $Br(HBr)_2^-$ and $Br(HBr)_3^-$ are shown in Figure 4.11. The harmonic calculations predict that (a) the addition of one HBr unit to the $BrHBr^-$

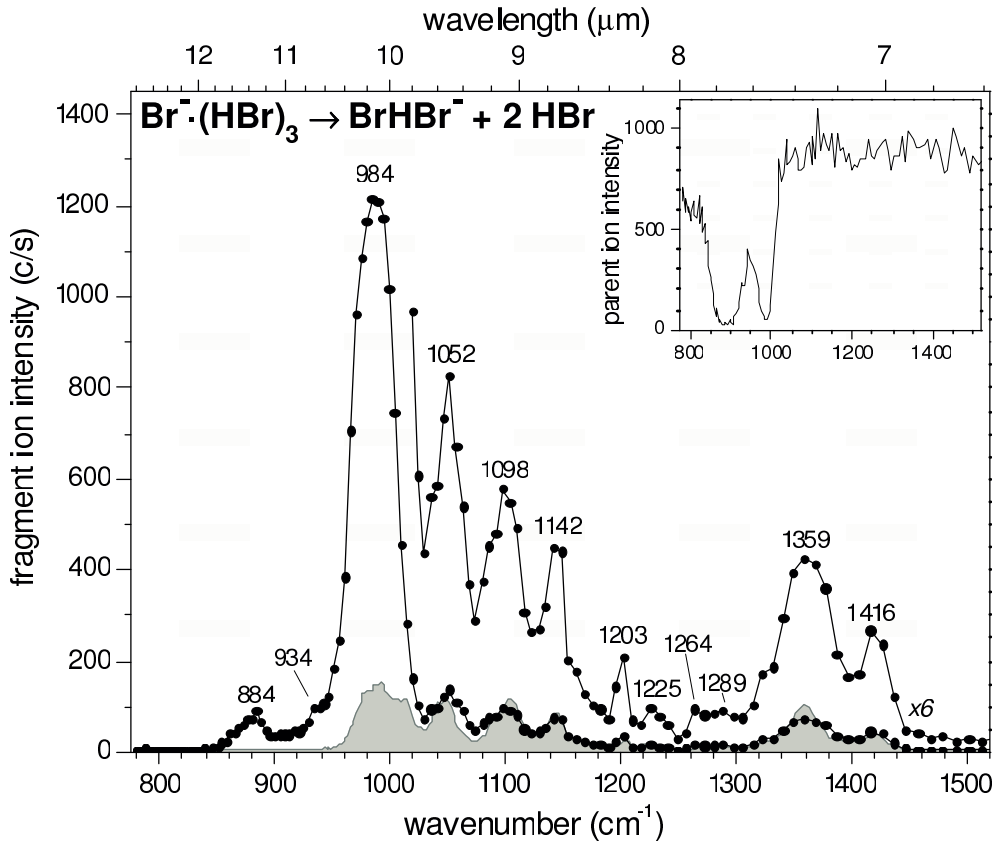

Figure 4.10: The infrared photodissociation spectrum of the $Br(HBr)_3^-$ anion for the second dissociation channel measured with 50 $mJ/macropulse$ laser pulse energy. The gray shaded area shows the IRPD spectrum of $Br(HBr)_2^-$. The inset present the parent ion depletion spectra.[73]

anion destroys the symmetry of the hydrogen bond and (b) the $Br - Br$ distance increases with 0.1 Å per additional HBr ligand. The calculated harmonic vibrational frequencies of the symmetric and the antisymmetric H-atom stretch of $Br(HBr)_2^-$ are 1453 and 1662 cm^{-1}, respectively. The two bands are relatively close to the peaks at 1359 and 1420 cm^{-1} in the experimental IR spectrum and therefore, these bands could be assigned to these two vibrational modes. Based on the reasonable isotope shift factors of 1.34 and 1.33, respectively, the peaks at 1014 and 1067 cm^{-1} in the $Br(DBr)_2^-$ spectrum can be assigned also to the symmetric and antisymmetric H-atom stretch. This assignment is supported also by the strong intensities of the two bands in $Br(DBr)_2^-$, but not by the intensities of the bands in $Br(HBr)_2^-$.

A second assignment can be given considering the breakdown of the harmonic approximation for strongly H-bonded systems (see previous section). Theoretically predicted frequencies (2364 cm^{-1}) for the antisymmetric H-atom stretch in $F(HF)_2^-$[88]

Table 4.5: Peak positions and normalized intensities for multiphoton dissociation of the $Br(HBr)_3^-$ anion.

parent ion	fragment ion	position (cm^{-1}) and normalized intensities
$Br(HBr)_3^-$	$Br(HBr)_2^-$	888 (1.00), 979 (0.16)
	$BrHBr^-$	884 (0.07), 934 (0.08), 984 (1.00), 1052 (0.11), 1098 (0.08), 1142 (0.06), 1203 (0.03), 1225 (0.01), 1264 (0.01) 1289 (0.01), 1359 (0.06), 1416 (0.04)

were experimentally observed at 1815 cm^{-1},[86] shifted by 549 cm^{-1}. Based on these observations, the peaks at 992 and 1048 cm^{-1} in $Br(HBr)_2^-$, which have the highest intensity, can be tentatively attributed to the symmetric and the antisymmetric H-atom stretches with corresponding peaks in $Br(DBr)_2^-$ at 761 cm^{-1} and 798 cm^{-1} (isotopic shifts of 1.3 and 1.31, respectively). The other bands in the spectra of $Br(HBr)_2^-$ can be tentatively attributed to combinations with the in-plane asynchronous H-atom wag and to the antisymmetric $Br - Br$ stretch which have harmonic frequencies predicted at 568 and 98 cm^{-1}, respectively, with low but non-zero intensities.[73]

For $Br(HBr)_3^-$ the harmonic calculated frequencies (1981 and 1807 cm^{-1}) are outside the measurement window and, thus, could not be observed. Considering the breakdown of the harmonic approximation, the absorption bands at 888 and 979 cm^{-1} from Figure 4.9 can be tentatively assigned to the fundamentals of the two H-atom stretch vibrations. The other bands in the region between 1000 and 1500 cm^{-1}, observed in the spectrum which was measured at higher laser intensity (Figure 4.10), are assigned to the photodissociation of $Br(HBr)_2^-$, which is formed in the trap by collision induced dissociation with the He buffer gas atoms.

While none of the presented assignments is satisfactory, both place the antisymmetric H-atom stretch at a higher frequency than the ν_3 fundamental of the $BrHBr^-$, providing an experimental evidence for the destruction of the symmetric hydrogen bond and localization of the H atom in the larger clusters as predicted by the harmonic calculation.[73] Photoelectron spectra measured for the $Br(HBr)_{2,3}^-$ systems[89] provide a second proof of the symmetric hydrogen bond distortion by addition of HBr ligands to the $BrHBr^-$ chromophore. This is evidenced by the broader peaks and with significantly larger spacing between these in $Br(HBr)_2{}^-$ than in $BrHBr^-$. The spacing between the peaks in the larger system is closer to the free HBr. According to this, the larger clusters can be defined as HBr ligands complexed to a

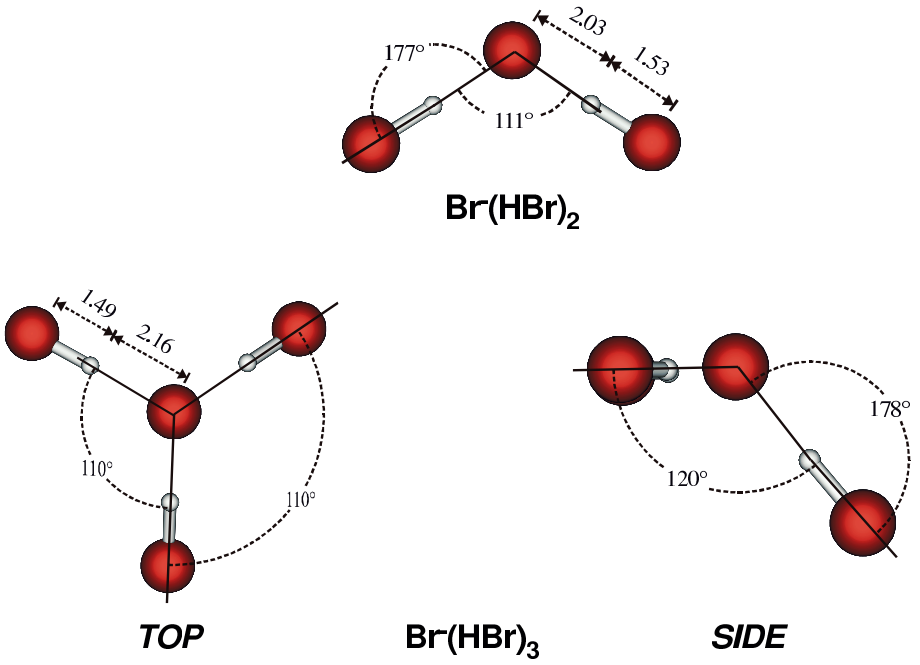

Figure 4.11: The C_{2v} structure for $Br(HBr)_2^-$ (above) and the C_{3v} structure for $Br(HBr)_3^-$ (below) (B3LYP/aug-cc-pVTZ method). (calculations performed by N. Pivonka[73]).

central bromide atom.

4.1.4 Conclusions

In this section, the IR spectra of strong hydrogen bonded $Br(HBr)_n^-$ (n=1-3) anions and of corresponding deuterized complexes was measured for the first time at the FELIX facility between 600 and 1700 cm^{-1}. Both multiphoton photodissociation and the messenger atom techniques were used and the results obtained from these two methods were compared to each other. $BrHBr^-$ is characterized by a symmetrically situated hydrogen atom between the two bromide atoms. The IR spectra of $BrHBr^-$ indicate a complete breakdown of the harmonic approximation already at low quantum numbers evidenced by the strong mode couplings between the symmetric and the antisymmetric stretching modes. The VPD spectrum of $BrHBr^- \cdot Ar$ shows an excellent agreement with theoretical anharmonic predictions. The IRMPD spectra are more complex showing additional structure. Based on the experience gained from the $BrHI^- \cdot Ar/BrHI^-$ systems, many of the additional peaks could arise from excitations to higher energy states via multiple photon transitions in which

two photons are resonant with one vibrational transition. IR measurements of the larger $Br(HBr)_n^-$ (n=2,3) anions indicate the distortion of the symmetric bond and the localization of the H-atom. Thus, the larger clusters can be defined as HBr ligands complexed to a central bromide atom. The VPD spectra of the studied systems originate most probably from singlephoton photodissociation, thus being closer to the linear absorption spectra which are usually predicted by theory. The IRMPD experiments require a high number of photons to reach the dissociation threshold, hence, a complete understanding of these spectra necessitate calculations which address the experiments directly.

4.2 Investigating the Vibrational Structure of Gas Phase Asymmetric Dihalogen Hydride Anions with Infrared Spectroscopy

Infrared spectra of the triatomic dihalides $BrHI^-$ and $BrDI^-$ have been previously investigated by matrix isolation spectroscopy.[90] The spectra revealed four bands at 666, 799, 920 and 1171 cm^{-1} for $BrHI^-$ and three bands at 470, 728 and 862 cm^{-1} for $BrDI^-$. Previous experiments on hydrogen dihalides in rare gas matrices[90,91] showed that depending on the experimental conditions two types of anions could be formed. The type I anions are characterized by an asymmetrically located hydrogen atom, leading to a high hydrogen stretching frequency. On the other hand, the type II anions are characterized by a more symmetric hydrogen position between the two halogen and a lower hydrogen stretching frequency than in the case of type I anions. According to these definitions, the bands at 920 and 1171 cm^{-1} in the $BrHI^-$ matrix spectra were assigned to the H-atom antisymmetric stretch and either to the fundamental or the first overtone of the bending mode in type I anions. The peaks at 666 and 799 cm^{-1} were assigned to the same vibrational motions in type II anions.[90]

D. M. Neumark and coworkers measured the gas phase photoelectron spectra of $BrHI^-$ and $BrHI^- \cdot Ar$.[92–94] The spectra revealed resolved vibrational structure which was close to the frequency of the diatomic HBr. This indicates that photodetachment of the anion reached the $I + HBr$ product valley of the neutral potential energy surface rather than the $[BrHI]^{\neq}$ transition state. The wave packet simulation performed by Bradforth *et al.*[92] using a simplified potential function for the anion and a model potential energy surface for the $Br + HI$ reaction produced a reasonable agreement with the experimental spectra for an antisymmetric hydrogen stretch frequency of 920 cm^{-1}. No satisfactory agreement was obtained when the value for the type II anion (666 cm^{-1})[90] was employed for the simulations. Given the approximations used in the calculations of Bradforth *et al.*,[92] this result alone does not constitute a definitive support for the type I anion in the gas phase.

CCSD(T) calculations performed by Kalendin *et al.*[95] for the gas phase $BrHI^-$ anion on a three dimensional (3D) potential energy surface predicted a linear geometry for $BrHI^-$ with the $H-Br$ distance shorter by 0.8 $\AA$ than the $H-I$. The calculated dissociation energy of 0.566 eV relative to the $I^- + HBr$ limit[95] is in good agreement with the experimental value of 0.698 eV.[81] Calculations of the vibrational energy levels yielded 1266.7 cm^{-1} for the antisymmetric hydrogen stretch ν_3. This frequency

is lower than the harmonic value of 1779 cm^{-1}, but 300 cm^{-1} higher than the matrix value of 920 cm^{-1} proposed for the type I anions.

The discrepancies between the matrix spectra[90] and the calculations[95] can be resolved by measuring the gas phase infrared spectra of these ions. These results will be presented in the following sections.

4.2.1 Experiment

The anions studied in the experiments presented here are generated with the electron impact source as described in Chapter 2. A gas mix of 0.5 % HBr in Ar for $BrHI^-$ and $BrDI^-$ and 0.05 % for the argon complexes $BrHI^- \cdot Ar$ and $BrDI^- \cdot Ar$ was used. This gas mixture is passed over a small quantity of methyl iodide which is allowed to evaporate in the gas line. The gas mix is expanded in the vacuum system through a pulsed valve running at 100 Hz. The hexadecapole ion trap was filled with 0.015 $mbar$ He for trapping and cooled to 16 K. The ions are trapped and intersected with the FELIX radiation. The trap was tipically filled for 150 ms for the experiments on the uncomplexed anions. For the Ar complexes longer filling times were necessary, due to the low ion intensities produced. For the experiments presented here, the FELIX macropulse had a duration of 7 μs. The bandwidth of the laser was 0.4 % of the central frequency (full width at half maximum) and had a maximum power of 300 mW at 5 Hz. One $ZnSe$ window and two KBr optics were in the laser beam previous to the interaction with the ions in the trap. Trapping of the argon complexes led to strong (80%) collision induced dissociation. In the case of the uncomplexed $BrHI^-$ and $BrDI^-$ anion, the IR spectra were measured by monitoring the I^- ion signal ($BrHI^- \rightarrow HBr + I^-$) as a function of the laser frequency, which led to background free measurements. Observation of a second dissociation channel, the loss of one HI unit ($BrHI^- \rightarrow HI + Br^-$) was also possible. However, the intensity of the Br^- signal was much lower than in the case of the I^- and showed no additional peaks in the spectrum. This is consistent with the stronger proton afinity of Br^- compared to I^-.

4.2.2 Predissociation Spectra

The predissociation spectra of $BrHI^- \cdot Ar$ and $BrDI^- \cdot Ar$ are shown in Figures 4.12 and 4.13. The measurements were carried out with step sizes of 0.04 μm. The values of the experimental vibrational frequencies are listed in Table 4.6. Compared to

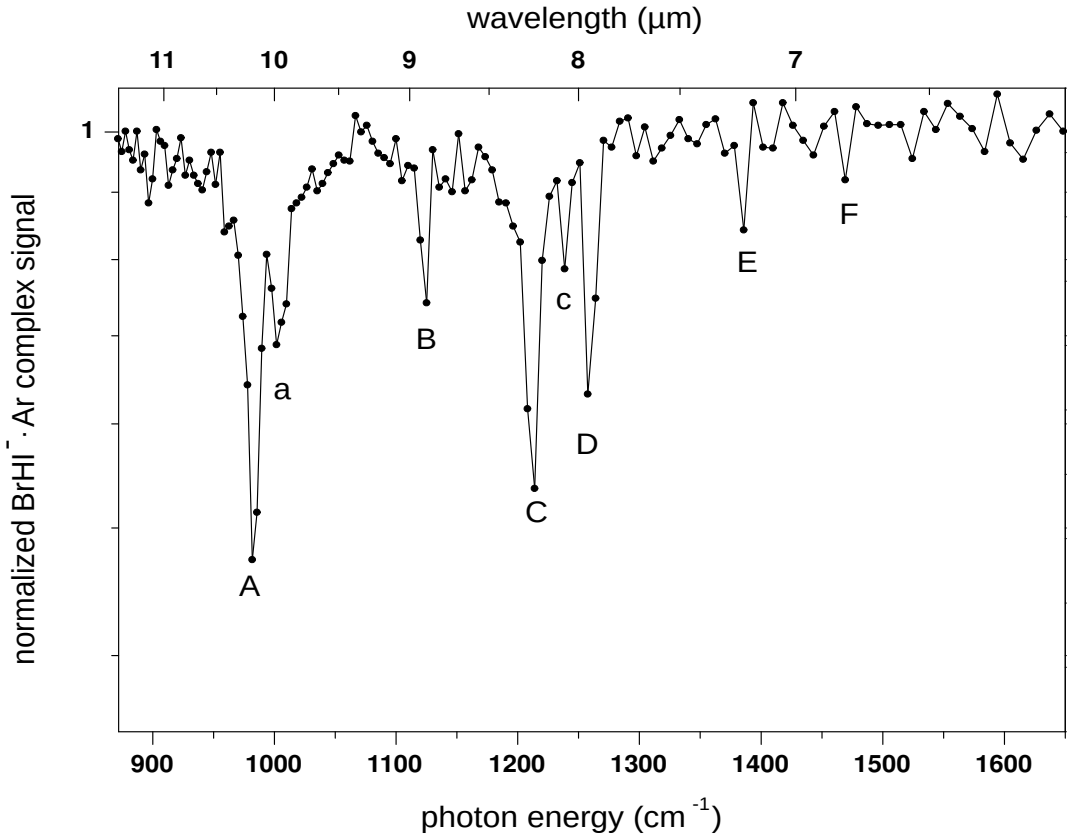

Figure 4.12: Infrared VPD spectrum of $BrHI^- \cdot Ar$ anion. The depletion signal of the $BrHI^- \cdot Ar$ complex is plotted on a logarithmic scale as a function of the laser frequency.[75]

the symmetric hydrogen dihalides presented previously in Section 4.1, the asymmetric systems show IR spectra with a higher complexity. In $BrHI^- \cdot Ar$ spectra six peaks are observed, labeled from A to F. Two additional peaks labeled a and c at a separation of $\approx 20\ cm^{-1}$ from peaks A and C are observed as well. The $BrDI^- \cdot Ar$ spectra show seven peaks labeled from A to I. The strongest intensity bands in both spectra are the peaks A and C at 948 and 1215 cm^{-1} for $BrHI^- \cdot Ar$ and 742 and 890 cm^{-1} for $BrDI^- \cdot Ar$. The separation between peaks A, B and D in the $BrHI^- \cdot Ar$ anion is 143 cm^{-1} and 132 cm^{-1}, respectively. The peaks A, B, D and F in the $BrDI^- \cdot Ar$ spectra are separated by 110 cm^{-1} and the peaks C, E and G are separated by 130 cm^{-1}.

The two strong bands A and C at 984 and 1215 cm^{-1} for $BrHI^- \cdot Ar$ and at 742 and 890 cm^{-1} for $BrDI^- \cdot Ar$ are close to the matrix values for the type I structure located at 920 and 1171 cm^{-1} for $BrHI^-$ and at 730 and 861 cm^{-1} for $BrDI^-$.[90] Hence, these bands could be attributed to the antisymmetric H-atom stretching vibration and to the fundamental or the first overtone of the bending mode.

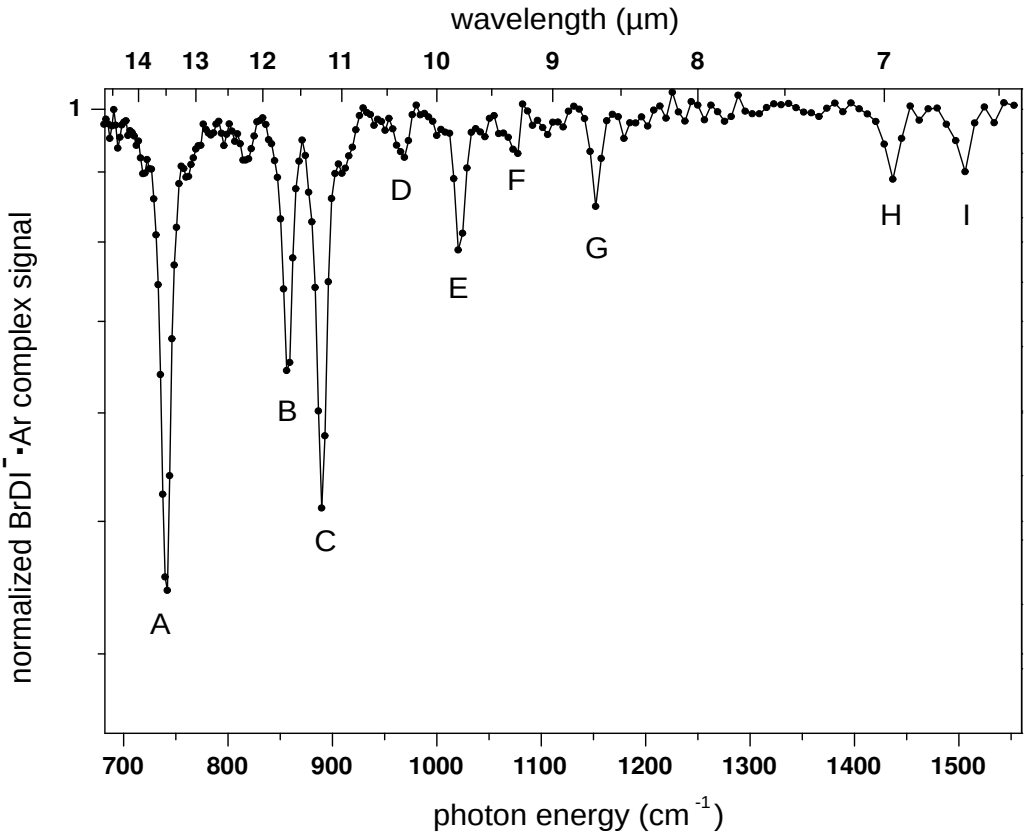

Figure 4.13: Infrared VPD spectrum of $BrDI^- \cdot Ar$. The depletion signal of the $BrDI^- \cdot Ar$ complex as a function of the laser frequency is shown on logarithmic scale.[75]

Kalendin *et al.*[95] predicted the antisymmetric stretch (001) and the first overtone of the bending mode (020) transitions in $BrHI^-$ at 1266 and 1026 cm^{-1}, respectively. The discrepancy between the matrix frequencies and theory suggests that the matrix spectra assignment needs to be revised. Furthermore, the question why the peaks A and C are comparable in intensity arises as well. Harmonic calculations predict the (001) transition more intense than the fundamental of the bending mode, let alone its overtone. Also no fundamental of the bending mode at half frequency value was observed in the gas phase or matrix spectra. Thus, the assignments of bands A and C to the (001) and (020) modes is questionable. Furthermore, no lower frequency bands which could be attributed to the type II structure are observed suggesting the existence of only one anion type in the gas phase. The separation between peaks A, B and D in the $BrHI^- \cdot Ar$ and between peaks A, B, D, and F and between C, E and G in the $BrDI^- \cdot Ar$ spectra indicates the existence of combination bands of the strong bands A and C with the symmetric stretch ν_1 which involves the vibration of the two halogen atoms. Similar to the assignment of the $BrHBr^- \cdot Ar$ VPD spectra,

Table 4.6: Peak assignment for VPD spectra of $BrHI^- \cdot Ar$ and $BrDI^- \cdot Ar$. ν_1, ν_2 and ν_3 represents the symmetric, bending and antisymmetric stretch modes. ν_{Ar} represents a vibrational motion involving the Ar atom.

	$BrHI^-$·Ar			$BrDI^-$·Ar		
	Peak position (cm^{-1})			Peak position (cm^{-1})		
Peak label	Experiment	Theory[a]	Assignment (ν_1 ν_2 ν_3)	Experiment	Theory[a]	Assignment (ν_1 ν_2 ν_3)
A	984	983.2	020+001	742	747.9	020+001
a	1003	···	(020+001)+ν_{Ar}			
B	1127	1126.9	120+101	857	864.2	120+101
C	1215	1228.0	020-001	890	910.5	020-001
c	1238	···	(020-001)+ν_{Ar}			
D	1259	1268.1	220+201	970	971.7	220+201
E	1380	1390.0	320+301	1021	1041.9	120-101
F	1468	1462.4	220-201	1080	1077.3	320+301
G				1154	1165.4	220-201
H				1433	1448.2	040+002
I				1502	1520.9	040-002

[a] - Reference[95]

peaks a and c, spaced by $\approx 20\ cm^{-1}$ from peaks A and C, respectively, are assigned to a rare gas atom mode.

Although many features of the IR spectra can be assigned, a better understanding of the position of the peaks and of the band intensities is achieved by theoretical analysis. The 3D potential energy surface (PES) and dipole moment, from which vibrational frequencies and intensities can be derived, have been calculated by J. M. Bowman and coworkers.[75] The multi-reference configuration interaction (MRCI) calculations were performed using the AVQZ basis set. For Br and I the Stuttgart effective core potential (ECP) was used. In Table 4.6, the calculated and experimental vibrational frequencies are presented and assignments for the peaks are given. The predicted infrared intensities are shown in Figure 4.14 and compared with the experimental VPD spectra.

The calculations predict a strong mode mixing between the bending and the H-atom stretching modes due to Fermi resonances. This mixing explains the comparable intensities of the peaks A and C, which were consequently assigned to the (020±001)

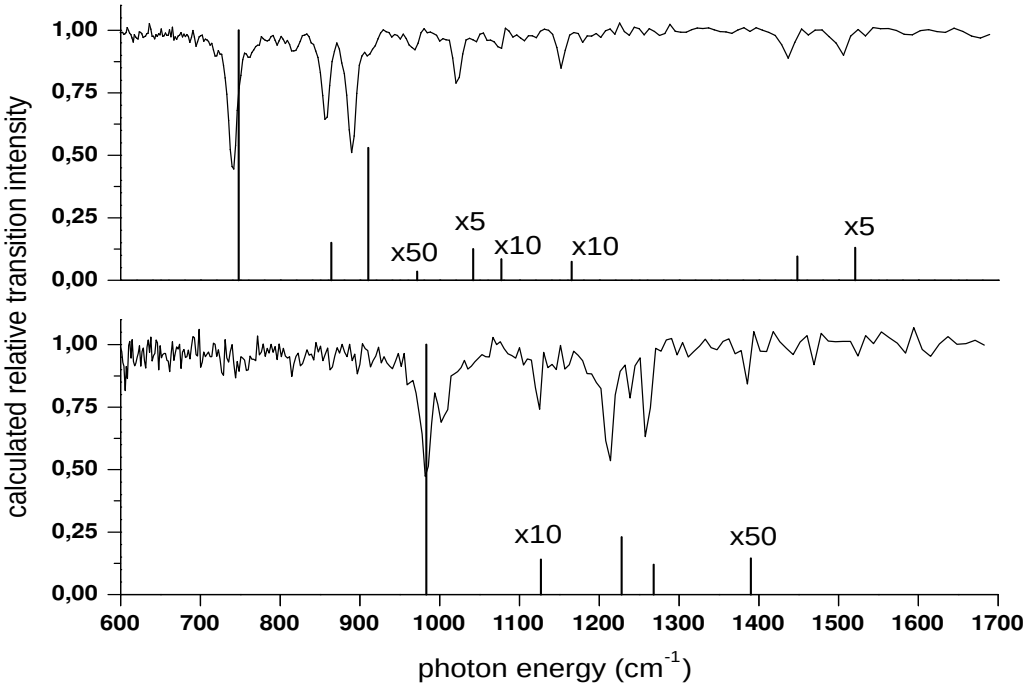

Figure 4.14: Comparison of the experimental predissociation spectra (black line) with the calculated frequencies and intensities (vertical bars). The upper panel shows $BrDI^-$; the lower panel shows $BrHI^-$. The experimental data are normalized to the background signal and shown on a logarithmic scale. Calculated intensities are normalized to the largest intensity and plotted on a linear scale for comparison.[75]

modes. A very good agreement between the theoretical vibrational frequencies and the experimental IR spectra is observed (see Table 4.6) which shows that the calculated PES[75] describes well the vibrational modes of the $BrHI^-$ and the $BrDI^-$ anions. The calculations support also the previous assignment that the peaks B, D, E and F for $BrHI^- \cdot Ar$ and the peaks B, D, E, F and G for $BrDI^- \cdot Ar$ are combination bands based on the peaks A and C with the low-frequency symmetric stretch ν_1. The calculations suggest the assignment of bands H and I from $BrDI^- \cdot Ar$ to the (040±002) transitions.

Although the position of the experimental infrared bands is in very good agreement with the theory, the intensities of the observed vibrational frequencies do not fit so well. Many of the smaller peaks are more intense in the VPD spectra than predicted by the calculations (see Figure 4.14).

The calculations predict as well that the transition strength of the (010) transition is comparable to the (001) transition, in contrast to the harmonic approximation. This is another consequence of the breakdown of the harmonic approximation for these complexes. The position of the fundamental of the bending vibration is calculated

at 597 and 427 cm^{-1} for $BrHI^-$ and $BrDI^-$, respectively. This suggests a new assignment of the bands at 666 cm^{-1} for $BrHI^-$ and at 470 cm^{-1} for $BrDI^-$ in the matrix spectra, which were attributed to the (010) mode of the type II structure.

The effect of the Ar atom was estimated by Bowman *et al.*[75] at the CCSD(T) level using the AVTZ basis set and the ECP for Br, I and Ar atoms. Three stationary structures were located with binding energies between 275 and 377 cm^{-1} (0.034 - 0.047 eV) indicating that only one photon is necessary to induce the dissociation of the Ar atom from the $BrHI^- \cdot Ar$ complex. A T-shaped geometry is found as global minimum geometry with the Ar atom closer to I than Br. The calculated shift for the bending and the H-atom stretch due to the Ar atom, for all three stationary points, are between 5 and 13 cm^{-1}.

4.2.3 Multiphoton Dissociation Spectra

The infrared spectra of $BrHI^-$ and $BrDI^-$ were investigated by the IRMPD technique as well. The multiphoton IR spectra for the $BrHI^-$ and $BrDI^-$ anions

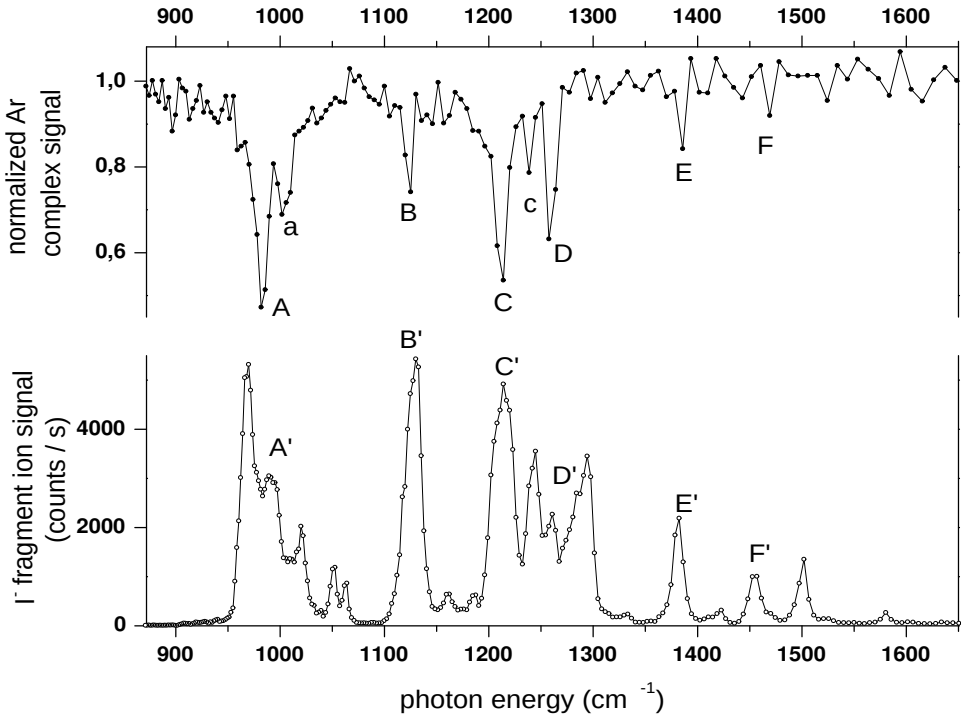

Figure 4.15: IR-VPD spectrum of $BrHI^- \cdot Ar$ (closed circles, upper trace) and the IRMPD spectrum of $BrHI^-$ (open circles, lower trace).[75]

are shown in the lower panel of the Figures 4.15 and 4.16. For comparison, the VPD spectra are shown in the upper panel. The peak positions are listed in Tables 4.7 and 4.8 for both anions.

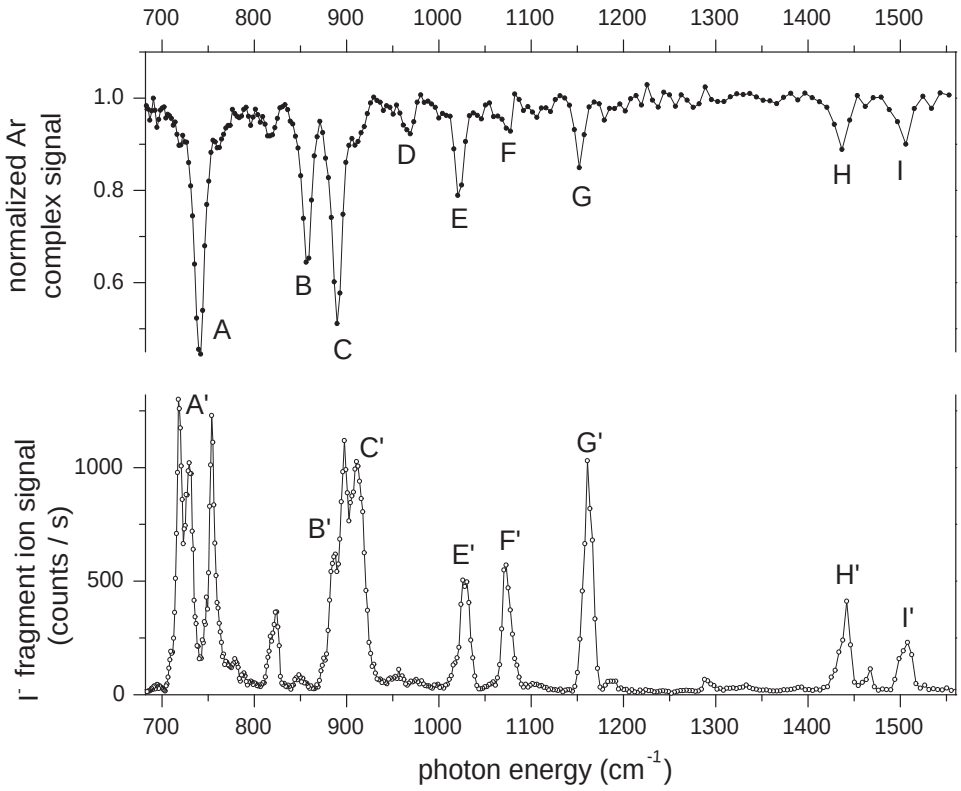

Figure 4.16: Infrared VPD spectrum of $BrDI^- \cdot Ar$ (closed circles, upper trace) and the IRMPD spectrum of $BrDI^-$ (open circles, lower trace).[75]

The VPD and IRMPD spectra are similar, however not identical. The similarities are underlined by the similar labels $A, B \cdots$ and $A', B' \cdots$ of corresponding bands. However, there are more peaks in the IRMPD spectra. Also, the smaller peaks in the VPD spectra are more intense in the IRMPD spectra. The bands at A and C appear as groups of closely spaced bands. By comparing the VPD with the IRMPD spectra shifts up to 30 cm^{-1} between pairs of corresponding peaks can be observed. In the frequency range where the spectra were recorded, 4 to 10 photons were necessary to be absorbed for dissociation. Differences between the VPD and the IRMPD spectra were observed in the case of the symmetric anions $BrHBr^-$ in Section 4.1 as well, however a better agreement can be identified here.

The groups of bands A' and C' could be attributed to transition from higher populated vibrational states (hot bands). However, the ions in the trap are cooled by

collisions with cold He atoms prior to the interaction with the laser beam and this possibility should be strongly reduced. Alternatively, the additional bands can be explained by multiple photon transitions in which two or more photons are resonant with one vibrational transition. In this case, the frequencies at which the excitation of these bands occurs would be shifted from the single-photon ones due to the anharmonicities in the anion. These multiphoton transitions would normally have a low intensity. However, FELIX peak intensity reaches up to 100 MW/cm^2 and resonant excitation to an overtone versus a fundamental could result in a more facile subsequent multiphoton absorption and dissociation.

Table 4.7: Peak positions and assignment for multiphoton dissociation of $BrHI^-$. Values in brackets are divided by two to show the expected two photon frequency. The assignments are given in the same manner as in the previous Subsection 4.2.2, where (ν_1 ν_2 ν_3) represent the symmetric, bending and antisymmetric stretching vibrations.

	Peak position (cm^{-1})			
Peak label	Experiment	Calculation[a] [÷2]	Assignment	Number of photons
A'	971	1939.3 [969.7]	040+002	2
	988	983.2	020+001	1
	1018	2035.6 [1017.8]	040-002	2
	1051	2107.9 [1054.0]	140+102	2
	1064	2123.4 [1061.7]	140-102	2
B'	1127	1126.9	120+101	1
	1162	2332.2 [1166.1]	240-202	2
	1187	2375.6 [1187.8]	340+302	2
C'	1213	1228.0	020-001	1
	1244	2445.2 [1222.6]	340+302	2
		2457.7 [1228.9]	021	2
D'	1262	1268.1	220+201	1
	1294	2599.6 [1299.8]	121	2
	1333	1339.0	120-101	1
E'	1382	1390.0	320+301	1
	1423	2857.0 [1428.5]	221	2
F'	1455	1462.4	220-201	1
	1498	1498.9 [1428.5]	420+401	1
	1580	1587.1 [1428.5]	520+501	1

[a] - Reference[75]

In order to explore the possibility of multiple photon transitions described previously, the energies of several vibrational levels of $BrHI^-$ and $BrDI^-$ lying at two times the frequency in the VPD spectrum were calculated and listed in Tables 4.7 and 4.8. Two photon absorptions are assumed and the photon energy at which each

level would be excited is given in the square brackets in both Tables 4.7 and 4.8. An excellent agreement between calculated and experimental frequencies for one photon transitions as well as for two photon transitions is observed. For example, the five experimental frequencies in the peak labeled as A' do not differ from the calculated values by more than 5 cm^{-1}. The assignment of some of the peaks in the high energy region becomes more difficult due to the low signal to noise ratio.

The assignments presented above attribute the intense peaks mostly to two photon rather than one photon transitions. For example in the case of the band at 971 cm^{-1} in the $BrHI^-$ spectrum which is attributed to a two photon transition although it has a higher intensity than the band at 988 cm^{-1} which is attributed to a one photon transition. As explained previously, the high intensity of these peaks can be due to a resonant excitation to an overtone from which subsequent multiphoton transitions are more facile than from the fundamental. The same effect is observed in the case of band H' at 1442 cm^{-1} in the $BrDI^-$ which is a one photon transition, but has a lower intensity as compared to the band A' at 719 cm^{-1} which is attributed to a two photon transition however in this case, the laser is three times less intense at 1440 cm^{-1} than at 700 cm^{-1}.

Another difference between the VPD and the IRMPD spectra is represented by the shifts between the corresponding pairs of peaks which are assigned to the same transitions. These shifts are larger at lower frequencies and seem to be more significant for the $BrDI^-$ than the $BrHI^-$ anion. The shifts in the $BrHI^-$ spectra due to Ar complexation are theoretically predicted to less than 13 cm^{-1}. These values are smaller than the experimentally observed shifts. The calculations were performed using the harmonic approximation and as it has been already discussed previously for the symmetric anions in Section 4.1, the harmonic approximation fails to describe quantitatively the strongly hydrogen bonded systems. However, qualitative estimates give an indication on the influence of the Ar atom. In the case of $BrDI^-$ anion, the shifts have values larger than 20 cm^{-1}. This makes the assignment of the peaks in the deuterized complex more difficult. An example is presented by the peak B for the $BrDI^-$ anion, which is assigned to the (120 + 101) transition. This band shows no shift in the $BrHI^-$ anion between the VPD and the IRMPD spectrum, but for $BrDI^-$ the shift is 29 cm^{-1} to higher values. This transition could be assigned as well to the band at 848 cm^{-1} where only a shift of 9 cm^{-1} is observed but to lower frequencies. However, the band at 848 cm^{-1} has a very low intensity to be assigned to an allowed one photon transition. It is not clear if the shifts can be attributed to the Ar complexation or to the IRMPD process, or a combination of both. However,

Table 4.8: Peak positions and assignment for multiphoton dissociation of $BrDI^-$. Values in brackets are divided by two to show the expected two photon frequency. The assignments are given in the same manner as in the previous Subsection 4.2.2, where (ν_1 ν_2 ν_3) represent the symmetric, bending and antisymmetric stretching vibrations.

	Peak position (cm^{-1})			
Peak label	Experiment	Calculation[a] [÷2]	Assignment	Number of photons
A'	719	1448.2 [724.1]	040+002	2
	730	747.9	020+001	1
	755	1520.9 [760.5]	040-002	2
	779	1582.9 [791.5]	140+102	2
	827	1645.3 [822.7]	140-102	2
	848	1691 [845.6]	240+202	2
B'	886	864.2	120+101	1
	900	1801.1 [900.6]	240-202	2
C'	911	910.5	020-001	1
		1819.9 [910.0]	021	2
	956	1939.4 [969.7]	121	2
		971.7	220+201	1
E'	1029	1041.9	120-101	1
F'	1073	1077.3	320+301	1
G'	1164	1165.4	220-201	1
	1188	1185.7	320-301	1
	1291	1305.5	420+401	1
H'	1442	1448.2	040+002	1
	1466	1429.3	420-401	1
I'	1509	1520.9	040-002	1

[a] - Reference.[75]

as it could be observed, the shifts between the VPD and the IRMPD spectra for the $BrHI^-$ anion are in the expected range for Ar complexation. This is different for the $BrDI^-$ anion and further studies are necessary to understand the origin of these shifts.

4.2.4 Conclusions

The VPD as well as the IRMPD spectra of the $BrHI^-$ and $BrDI^-$ anions was measured for the first time at the FELIX facility in the region of the H-atom stretches. The spectra reveals strong couplings between all vibrational modes. Based on the combination of the experimental results with high level calculations,[75] previous assignments of the matrix spectra were revised. No indication of the type II anions was

observed in the gas phase. The band positions in the VPD spectra are in excellent agreement with theoretical predictions. Furthermore, the high level calculations of Bowman *et al.*[75] manage to decipher all the peaks in the IRMPD spectra based on possible two photon absorptions which are resonant with one vibrational transition. Such high level calculations extended in the frequency range above the monitoring window of the experiment might possibly explain the groups of peaks in the IRMPD spectra of $BrHBr^-$, based again on the consideration of multiple photon transitions to higher energy states. Questions concerning the intensity of the bands and the shifts in the $BrDI^-$ anion between the VPD and IRMPD peaks assigned to the same transitions remain open and hopefully will stimulate further studies.